Journal of Applied Sciences

ISSN 1812-5654

science alert

ANSInet
an open access publisher
http://ansinet.com

Journal of Applied Sciences 11 (20): 3482-3489, 2011
ISSN 1812-5654 / DOI: 10.3923/jas.2011.3482.3489
© 2011 Asian Network for Scientific Information

Investigation of Rolling Loss Mechanisms in Plastic Optical Fibers

H. Golnabi and N. Aghighi
Department of Physics, Islamic Azad University, Tehran North Branch, Tehran, Iran

Abstract: A simple opto-mechanical system is introduced to monitor the fiber bending effects. Investigation of fiber rolling loss mechanisms in plastic optical fiber by intensity modulation of the transmitted light is reported. The transmitted light powers in the plastic fibers in bend-free and under bending deformation are measured and compared. By reducing the bending diameter (from 18 cm to 7.33 cm) the bending power loss is increased, accordingly. For the green LED for the force-free case the transmitted power is 7456.0 nW, while for bending diameter of 18 cm is 7349.8 nW, for bending diameter of 15 cm is 7291.4 nW, for bending diameter of 9.82 cm is 6687.6 nW and finally for the bending diameter of 7.33 cm is decreased to 5863.6 nW. For all the measurements the green LED shows the highest transmitted power while the red LED shows the lowest output power. Theoretically, the critical bending radius is computed as a function of the core index of refraction for a fixed value of the cladding index of refraction for different core radii. For the core radius of 430 μm the critical bending radius is about 12 cm, while for the core radius of 50 μm it is reduced to 1.8 cm. For a fixed refractive index of the cladding (1.43), the critical bending radius is decreased by increasing the core refractive index (1.44-1.52). The reported system provides a simple and accurate means for the bending loss investigation of fibers even for large-diameter bending cases.

Key words: Bending effect, deformation force, total reflection, transmission loss

INTRODUCTION

Light guides are transparent devices that conduct the flow of light from a source to the point of interest and optical fibers are one of the most effective links in this respect. In recent years a variety of experimental and theoretical investigations have been made to study the bending loss mechanisms in different fibers and fiber cable transmission lines (Baptista *et al*., 2006; Babchenko and Maryles 2007; Senior, 1985). A Plastic Optical Fiber (POF) has a transparent inner core and a thin exterior cladding and a protective sleeve. Typically, POF has a continuous operating range of -55°C to 70°C and can withstand up to 100°C for a short period of time less than 1 min. Silica glass optical fiber has a better light transmission characteristic (less loss) than POF and can tolerate higher temperatures than plastic fibers. However, POFs are more flexible, less problems to fabricate into special assemblies and lower in cost than glass fibers (Zubia and Arrue, 2001; Levi, 1980). The typical white light attenuation in POF is 0.2 to 0.25 dB mm^{-1}. Light guides and scanners often using the POFs for the beam shaping (Asadpour and Golnabi, 2008, 2010) and light transmission are reported (Jafari and Golnabi, 2008; Haghighatzadeh *et al*., 2009; Entezari and Golnabi, 2011; Khorramnazari and Golnabi, 2011). POFs can be used for sensing operations as well (Golnabi and Jafari, 2006; Jafari and Golnabi, 2010).

The main objective of this study was to introduce a simple and sensitive opto-mechanical system in order to investigate the fiber bending effects. For this purpose in the first section of this report the fiber bending losses are described.

FIBER BENDING LOSSES

A general theory, which considers the solution of the wave equation propagating in the optical fibers is given (Van Etten and Plaats, 1991). Optical fibers suffer certain losses at bends or curves on their propagation path. Bending losses in fibers can be considered as microbend (tight-diameter bend) and macrobend (large-diameter bend) losses and can result losses of the transmitted power. Microbend losses are associated with the small perturbations of the fiber for example induced by factors such as uneven coating application or cabling-induced stresses (centimeter in radius). Microbend losses may be a function of temperature and installation stresses or pressure on the fiber. Macrobending affects the lesser-confined modes due to fiber bending in the fiber

Corresponding Author: Hossein Golnabi, Department of Physics, Islamic Azad University, Tehran North Branch, P.O. Box 11155-8639, Tehran, Iran Tel: +982166164126 Fax: +982166164651

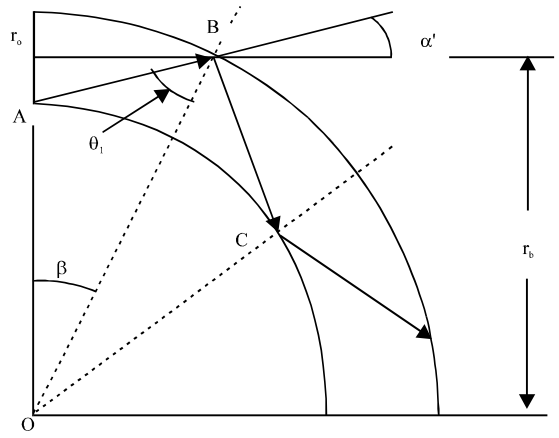

Fig. 1: The geometrical arrangement for a bend fiber

waveguide. Due to bending the evanescent fields reach into the cladding and thus can be affected by the distortion of the cladding as well as core. The result of the microbend perturbation is to cause the coupling of the propagating modes in the fiber by changing the optical path length and the multimode fiber loss from random bends is given by Allard (1990):

$$M_L = N(h)^2\left(\frac{a^4}{b^6\Delta^3}\right)\left(\frac{E}{E_F}\right)^{3/2} \quad (1)$$

where, M_L is multimode loss; N is number of bumps per unit length; h is average height of the bump; b is fiber diameter; a is fiber core radius; E_F is elastic modules of the fiber; E is elastic modulus of the surrounding medium and Δ is index difference between the core and cladding. From Eq. 1 increasing the refractive index of the core decreases the fiber's sensitivity to such a bending loss. Increasing overall fiber diameter also decreases sensitivity while increasing core diameter increases the sensitivity. The loss of the higher modes causes a gradual increase in multi-mode fiber attenuation.

Consider a fiber with the cross sectional core radius of r_0, which is bended to a circular form with a radius of r_b where the center of the bend is point O as shown in Fig. 1. The optical axis passing through the center of the core circle as shown in Fig. 1 is point O. The first reflection angle at the first bend point B in Fig. 1 is given by:

$$\sin\theta_1 = \frac{(r_b - r_0)\cos\alpha'}{r_b + r_0} \quad (2)$$

where, angle α' is the angle between the incident ray and horizontal axis. The optical path by the light from the point A and the first total reflection point B (line AB) in the bend fiber is given by:

$$\Delta S = (r_b + r_0)\frac{\sin\beta}{\cos\alpha'} \quad (3)$$

where, angle β is the angle of the line OB with respect to line OA and the ratio of the beam path with the related length of the fiber is:

$$\frac{\Delta S}{\Delta L} = \frac{r_b + r_0}{r_b}\frac{\sin\beta}{\beta\cos\alpha'} \quad (4)$$

If we define:

$$\rho = \frac{r_0}{r_b} \quad (5)$$

then we have:

$$\frac{\Delta S}{\Delta L} = (1+\rho)\frac{\sin\beta/\beta}{\cos\alpha'} \quad (6)$$

The critical bending ratio is then given by:

$$\rho_c = \frac{n_1 - n_2}{n_1 + n_2} = \delta/2 \quad (7)$$

where n_1 is the refractive index of the core material and n_2 for cladding and we assume average index of the refraction to be:

$$\bar{n} = \frac{n_1 + n_2}{2} \quad (8)$$

and the relative index of refraction difference is given by:

$$\delta = \frac{n_1 - n_2}{\bar{n}} \quad (9)$$

One can say that by bending the fiber, Numerical Aperture (NA) is reduced to the value given by (virtual numerical aperture):

$$A_b = n_0\sin\alpha_{max\,b} = \left[n_1^2 - n_2^2\left(\frac{1+\rho}{1-\rho}\right)^2\right]^{1/2} \quad (10)$$

and it is equivalence to an increase in the refractive index value of the cladding n_2 by a factor of:

$$\frac{1+\rho}{1-\rho} \quad (11)$$

and whenever this factor is less than ratio of n_1/n_2 then the relating beam incident into the optical axis escapes from the fiber due to such a bending effect. From Eq. 6 the critical bending radius for ray launched on optical axis can be obtained from the following relation:

$$(r_b)_c = r_0 \frac{n_1 + n_2}{n_1 - n_2} \quad (12)$$

where all the quantities are defined before. As can be seen in Eq. 12 where the core radius is increased the critical bending radius is increased accordingly and by decreasing the index of refractive difference factor the critical bending radius is also increased. For a radius given equal or smaller than the value given by Eq. 12 the incident ray is escaping from the fiber wave guide, which causes the bending loss effect.

According to Fig. 1, the given formulas are for the case of a ray parallel to horizontal axis on the optical axis of the figure just incident on the center part of the fiber core section. For a parallel ray with the height of h from such optical axis the governing relation mentioned as Eq. 2 is replaced by:

$$\sin\theta_1(h) = \frac{(r_b + h)\cos\alpha'}{r_b + r_0} \quad (13)$$

where, we have $-r_0<h<r_0$ and the rest of equations described remain unchanged. From given discussions it is obvious that for small index difference even a small bend in the fiber causes that particular beam to escape from the guiding fiber. Thus for such conditions for small microbend situation of the fiber from straight line position will cause loss of such beams. For the case that there are many of such microbending points in the fiber length this effect will cause a considerable loss in transmitted beam power (Allard, 1990; Crisp and Elliott, 2005).

Wavelength of the incident beam also affects the macrobend losses in a fiber. In general such a bend loss can be considered as the radiation attenuation coefficient, which is given by:

$$\alpha_T = c_1 \exp(-c_2 r_b) \quad (14)$$

where, r_b is the radius of curvature of the fiber bend and parameters c_1 and c_2 are constants (Senior, 1985; Allard, 1990). Large or macrobending losses tend to occur in multimode fibers at a critical radius of curvature $(r_b)_c$, which may be obtained from:

$$(r_b)_c = \frac{3n_1^2\lambda}{4\pi(n_1^2 - n_2^2)^{1/2}} \quad (15)$$

where, n_1 and n_2 are the refractive index of the core and cladding materials, respectively. As can be seen in Eq. 15, shorter wavelength light implies a lower critical bend radius and also smaller index difference is more suitable for less bending loss effect as described in the previous section.

EXPERIMENTAL METHOD

The basic experimental arrangement used in this research is shown in Fig. 2a, which consists of a light source, a transmission fiber, a mechanical device for fiber deformation generation and a light power meter for power monitoring. Figure 2a shows the principle of experiment where a multimode plastic fiber is used for the output power modulation experiment. The light source can be either a coherent laser light, white or color LED, or a white filament lamp. The light sources used here are either a white LED or a color light LED all operating at a supply voltage of 5 V for a better comparison. The Plastic Optical Fibers (POFs) as described can operate successfully at visible wavelength range and thus such light sources used in this experiment (Zubia and Arrue, 2001; Mohanty and Kuan, 2011).

Since, the cross section of the fiber is large enough, therefore, the source light is directly coupled to the fiber. The POF used here are effective but, better fibers and a better treatment of the fiber ends can improve the coupling efficiency of the fiber to source and finally to photodetector. The overall diameter of this multi-mode fiber is about 2.2 mm with a cladding diameter of about 1 mm and the core diameter of about 0.860 mm. The fiber length used here is about 7 m. One end of the transmission fiber is connected to the LED light source and the other end is connected to the power meter for

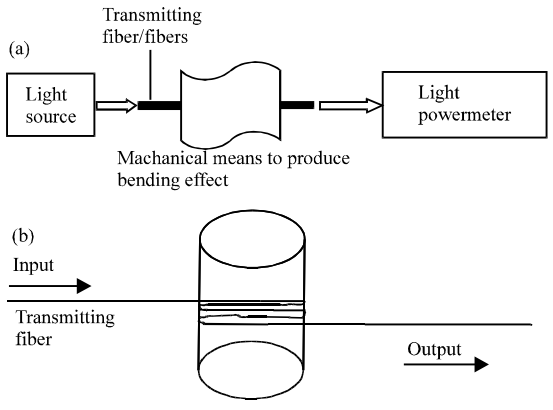

Fig. 2: Block diagram of the experiment (a) and (b) cylinder for the rolling effect

power monitoring. In this experiment to roll the fiber a cylindrical piece as shown in Fig. 2b is used and the fiber is rolled tightly around its surface. By using different cylinders with different diameters it is possible to generate different bending diameters for the measurement. Since the fiber length is fixed by reducing the cylinder diameter the number of turns are increased, respectively. For this experiment four different cylinders are used to provide the bending diameters of 18, 15, 9.82 and 7.33 cm for the rolled fiber.

EXPERIMENTAL AND THEORETICAL RESULTS

For a more consistent operation of the LED light source, in the initial experiment the variation of the output power as a function of the supply voltage is investigated. Fig. 3 shows the variation of the light source power as a function of the supply voltage. As can be seen the power behavior is different for the supply voltage range of 3-3.5 V but for the range of 4-5 volts the response is linear with a smooth increase. Thus supply voltage of 5 V is used through all the reported experiments for the LED light sources. All the experiments for the given light sources are performed at the similar source-fiber coupling arrangement and for uniform illumination intensity at such a fixed power supply voltage.

In the first study for the initial reference the power transmission for the fiber is measured where there is no bending deformation along the fiber length. As can be seen in Fig. 4, experiments are performed for the green, orange, white and red LED light color sources. For comparison the supply voltage for the LEDs are kept similar at 5 V level. Vertical axis shows the transmitted power for the tested plastic fiber for the different light colors and for a better comparison the values are shown on the graph bars in Fig. 4. For the tested LEDs the green LED shows the highest transmitted power (7456.0 nW) while the red LED shows the lowest transmitted power (5317.2 nW).

In the next experiments a cylinder as shown in Fig. 2b is used to roll the same fiber. By using different cylinders with different diameters it is possible to generate different bending diameters for the measurements. Since the fiber length is fixed by reducing the cylinder diameter the number of rolled turns is increased, accordingly. For this experiment results for the bending diameters of 18, 15, 9.82 and 7.33 cm are reported. Power modulation for the rolled fiber with bending diameter of 18 cm (number of turn equal to 10) for different LED light colors is shown in Fig. 5. As indicated the vertical axis shows the transmitted power for the tested plastic fiber for the different light colors and for a better comparison the power values are

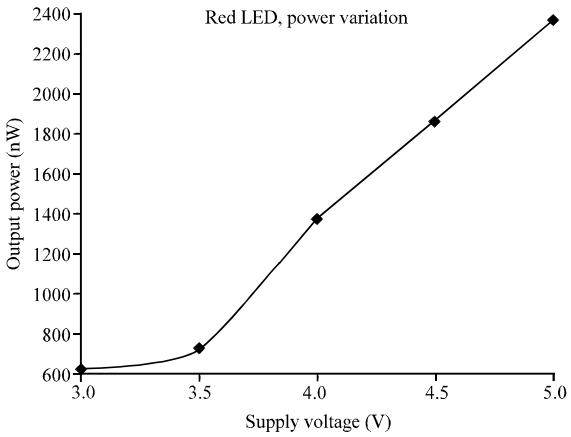

Fig. 3: Variation of the light source as a function of supply voltage

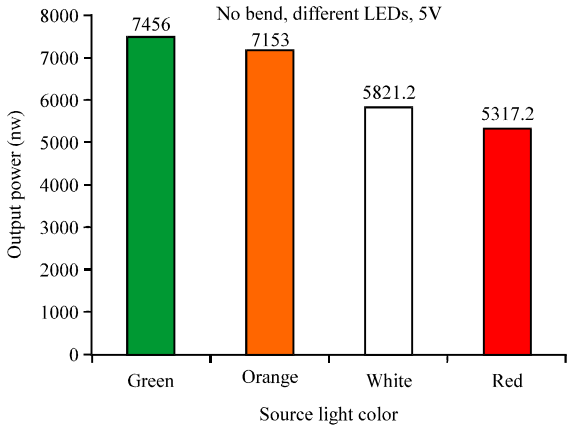

Fig. 4: Output powers of a fiber with no bending effect for different LED light colors

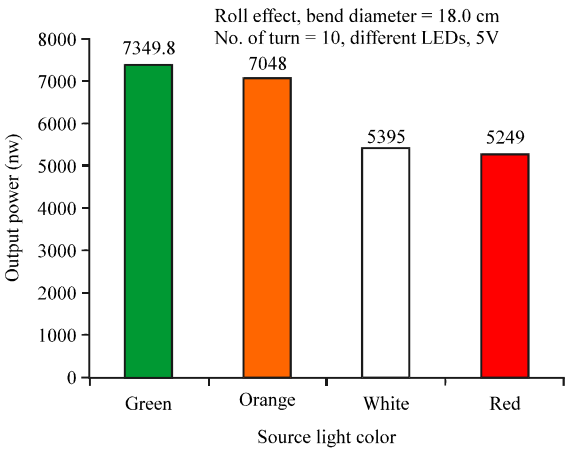

Fig. 5: Power modulation of a rolled fiber with bending effect (n = 10 turn, d = 18 cm) for different LED light colors

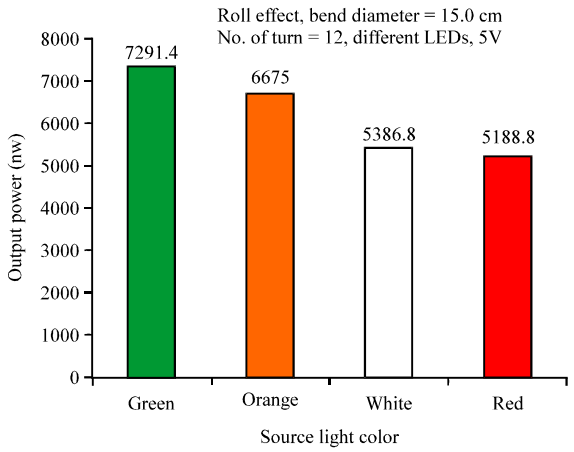

Fig. 6: Power modulation of a rolled fiber with bending effect (n = 12 turn, d = 15 cm) for different LED light colors

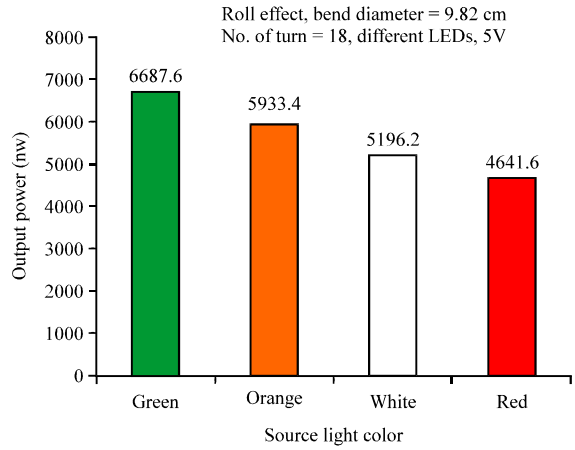

Fig. 7: Power modulation of a rolled fiber with bending effect (n = 18 turn, d = 9.82 cm) for different LED light colors

shown on the graph bars in Fig. 5. For the tested LEDs the green LED shows the highest transmitted power (7349.8 nW) while the red LED shows the lowest transmitted power (5249.0 nW). In the next investigation results of the power modulation for the plastic fiber with bending diameter of 15 cm and a number of turns equal to 12 for different LED light colors are shown in Fig. 6. For example, for the tested LEDs the green LED shows the highest transmitted power (7291.4 nW) while the red LED shows the lowest transmitted power (5188.8 nW).

Next experiment considers the results of power modulation for the plastic fiber with the bending diameter of 9.82 cm (number of turns equal to 18) for different LED light colors as shown in Fig. 7. The transmitted powers for

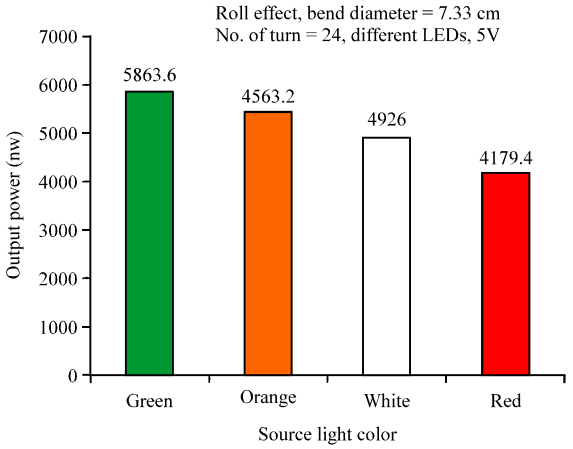

Fig. 8: Power modulation of a rolled fiber with bending effect (n = 24 turn, d = 7.33 cm) for different LED light colors

the tested plastic fiber for the different light colors are shown. For example, for the tested LEDs the green LED shows the highest transmitted power (6687.6 nW) while the red LED shows the lowest transmitted power (4641.6 nW). Last experiment considers results of the power modulation for the plastic fiber with bending diameter of 7.33 cm (number of turns equal to 24) for different LED light colors. As usual as shown in Fig. 8, the vertical axis shows the transmitted power for the tested plastic fiber for the different light colors and for a better comparison the values are indicated on the graph bars in Fig. 8. For instance, for the tested LEDs the green LED shows the highest transmitted power (5863.3 nW) while the red LED shows the lowest amount of the transmitted power of 4179.4 nW.

Now it is constructive to study theoretically the bending process for the rolled fiber. Thus, in the last study the effect of the macro-bending is investigated. Based on Eq. 12 the critical bending radius is computed by a Matlab program as a function of the core index of refraction for a fixed value of the cladding index of refraction. As can be seen in Fig. 9, the critical bending radius depends on the fiber core radius and such computations are performed for three different fiber core sizes. By decreasing the core radius the critical bend radius is decreased, accordingly. For example for 430 μm the critical bending radius is about 12 cm, for r = 200 μm is reduced to 5.5 cm and finally for the r = 50 μm is about 1.8 cm. This means that for bending radius less than the given critical values, the fiber experiences power losses under macro-bending condition. As can be seen in Fig. 9, for the fixed refractive index of the cladding (1.43), the critical bending radius is decreased by increasing the core refractive index.

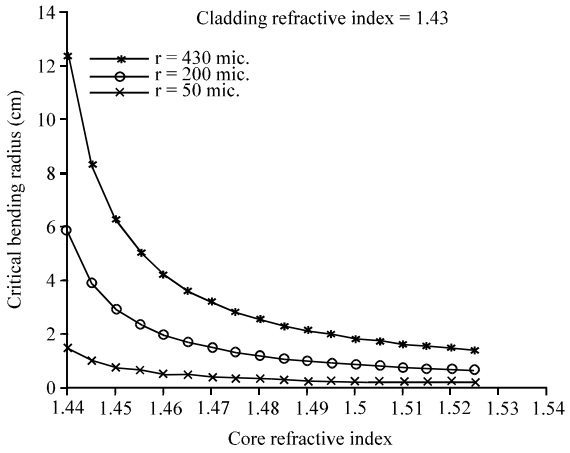

Fig. 9: Critical bending radius as a function of the core index of refraction for a fixed value of the cladding index of refraction for different core radii

However, for the assumed values such drop in radius strongly depends on the refractive index difference and for Fig. 9, a sharp drop is noted for the core refractive index of 1.44 to 1.47. When the difference in the index of refractions is very large the variation is very slow and the critical bending radius is almost constant. In term of the critical optical bending radius (case that total reflection fails), for the case of core refractive index of $n_1 = 1.5$, cladding index of $n_2 = 1.48$, from Eq. 12 the critical bending radius is 6.4 cm. For the fixed core radius of 430 m, when the index difference term is 0.01 (1.44-1.43) the critical bending radius is 12 cm, while for index difference of 0.02 (1.5-1.48) the critical bending radius is reduced to 6.4 cm.

DISCUSSION

Figure 4-8 are good bases for the comparison purposes and three major points can be discussed from the given results. First, for the no bending situation and all the bending cases the trend of the power transmission variation is the same. For all the measurements the green LED shows the highest transmitted power while the red LED shows the lowest output power. Second and perhaps the more important one, when there is no perturbing bending force the amount of the transmitted power as expected is the highest value for all the illumination source light colors. For a given source light, by reducing the bending diameter the power loss is increased, accordingly. For example, for the green LED for the case of force-free the transmitted power is 7456.0 nW, while for bending 18 cm diameter is 7349.8 nW, for 15 cm bending diameter is 7291.4 nW, for 9.82 cm bending diameter is 6687.6 nW and finally for the bending diameter of 7.33 cm transmitted power is decreased to 5863.6 nW. Third point is that at first look the power loss comparison for different launching light color shows the green transmitted light is higher than for the other colors. However, this does not mean that there is a lower attenuation for the green light as a result of the bending forces for the fiber. For this case the fact is that the green LED has a higher output and as a result the fiber input power for this source is higher than those of the other sources. A more precise analysis for this case requires different color LEDs with the compatible output powers for a better comparison.

Now it is useful to consider the theoretical results in the following discussions. As stated, the critical bending radius depends on the fiber core radius. By decreasing the core radius the critical bend radius is decreased, accordingly. For example for 430 μm the critical bending radius is about 12 cm, for r = 200 μm is reduced to 5.5 cm and finally for the r = 50 μm is about 1.8 cm. For the fixed refractive index of the cladding (1.43), the critical bending radius is decreased by increasing the core refractive index. Such decrease in radius strongly depends on the refractive index difference and a sharp drop is noted for the core refractive index of 1.44 to 1.47. When the difference in the index of refractions is very large the variation is very slow and the critical bending radius is almost constant. In term of the critical optical bending radius (case that total reflection fails), for the case of core refractive index of $n_1 = 1.5$, cladding index of $n_2 = 1.48$, the critical bending radius is 6.4 cm.

For the fixed core radius of 430 m, when the index difference term is 0.01 (1.44-1.43) the critical bending radius is 12 cm, while for index difference of 0.02 (1.5-1.48) the critical bending radius is reduced to 6.4 cm. The critical bending radius depends on the fiber core radius, where by decreasing the core radius the critical bend radius is decreased, accordingly. For the core radius of 430 μm the critical bending radius is about 12 cm, while for the r = 50 μm is reduced to only 1.8 cm. For a fixed refractive index of the cladding (1.43), the critical bending radius is decreased by increasing the core refractive index.

As a result of this study when the difference in the index of refractions is very large the critical bending radius variation is very slow and the critical bending radius is almost constant. For a fiber with the low value of the critical bending radius it means that such a fiber can be bended to a small radius at the expense of a lower power loss, while for the high value of the critical bending radius power loss occurs even for the high bending cases. As can be seen in theoretical results by decreasing the bending radius below the critical value the numbers of the escaped rays at the interfaces are increased and as a result the output power is reduced. When the bending

radius is smaller than the critical bending radius the escape of the incident rays at the interfaces is enhanced and more power is lost at the interfaces. This is in agreement with the experimental results for the fiber output measurements. When the bending radius is decreased the amount of the power loss is increased and as a result as shown in Fig. 5-8 the measured transmitted power is decreased accordingly.

As described in literature many attempts have been made to reduce the fiber bending losses. Hole-Assisted Fiber (HAF) is an attractive light-guide method with small bending losses. Such a design of fiber is unique because of the air holes in the cladding part of the fiber materials. Its characteristics are realized simply by introducing several air holes into a conventional fiber with a specific refractive index profile (Ieda *et al*., 2008). Design and characteristics of single-mode and low bending loss HAF are investigated both numerically and experimentally. They introduced an air filling fraction S and clarified the S dependence of the bending loss and the cutoff wavelength. They showed that HAFs with the desired parameter values can be designed roughly by taking account of the S dependence and the relative index difference dependence. Their results reveal that HAF with a loss of less than 0.1 dB/turn at 1625 nm and with a 5 mm bending radius can be achieved while maintaining transmission characteristics comparable to those in conventional single mode fibers.

In another study characteristics of bending loss optimized hole assisted fiber is described (Nakajima *et al*., 2010). That paper describes the transmission characteristics of a HAF, which has a conventional germanium-doped core surrounded by several air holes. They reported the design principle of the HAF in terms of both bending loss and mode-field diameter characteristics. Their results show that bending loss optimized HAF will be useful for constructing a flexible optical network. Our experimental results revealed that the reported system here can be used to measure the fiber bending loss for the conventional fiber arrangement and for the fabricated HAFs. As indicated by many articles designed single-mode and low bending loss HAFs are beneficial for constructing future networks and the bending loss measurement is an important issue.

CONCLUSIONS

It was shown that intensity modulation technique can be used in a perturbing design in order to obtain information about bending losses in plastic fibers. The following main points can be concluded from our results. First, the fiber dimension and materials are important in bending loss mechanisms. Second, the roll effect is more pronounced in the fiber with smaller bending diameter. Third, the light wavelength and the nature of the deformation of the fiber play important roles in the mechanism and as a result in power loss. The experimental arrangement used here effectively shows the phenomenon of the bending losses. Experimental results verify that the reported arrangements can be effectively used to monitor the modulated transmitted intensity caused by such mechanical perturbations in the fiber waveguide.

Considering the theoretical results, for a fixed value of the fiber refractive index of the cladding, the critical bending radius is decreased by increasing the core refractive index. When the difference in the index of refractions ($\triangle n = n_1 - n_2$) is very large the critical bending radius variation is very slow and the critical bending radius is almost constant. By decreasing the bending radius the numbers of the escaped rays at the interfaces are increased and as a result the output power is reduced. This is in agreement with the experimental results for the fiber output measurements. When the bending radius is decreased the amount of the power loss is increased and as a result the measured transmitted power is decreased, accordingly.

Using the reported techniques one can extract information concerning the nature and amount of power losses in optical fibers with a good precision. Obtained results show that the reported system provides a simple and accurate means for the bending and rolling loss investigations of the plastic optical fibers even for large-diameter bending cases with the minor deformation losses. In order to compare and verify the experimental results a theory for the critical bending radius is developed and there is a good agreement between the two results. As a result, the reported method can be used for the bending loss monitoring for both the single and multi-mode fibers. The results reported here are for the multimode plastic fibers but can be used for the conventional or modified single-mode fibers of other fabricated fibers with different materials and core-cladding arrangements.

REFERENCES

Allard, F.C., 1990. Fiber Optics Handbook for Engineers and Scientists. McGraw-Hill, New York, USA., Pages: 549.

Asadpour, A. and H. Golnabi, 2008. Beam profile and image transfer study in multimode optical fiber coupling. J. Applied Sci., 8: 4210-4214.

Asadpour, A. and H. Golnabi, 2010. Fiber output beam shape study using imaging technique. J. Applied Sci., 10: 312-318.

Babchenko, A. and J. Maryles, 2007. Graded-index plastic optical fiber for deformation sensing. Opt. Lasers Eng., 45: 757-760.

Baptista, J.M., S.F. Santos, G. Rego, O. Frazao and J.L. Santos, 2006. Micro-displacement or bending measurement using a long-period fibre grating in a self-referenced fibre optic intensity sensor. Opt. Commun., 260: 8-11.

Crisp, J. and B.J. Elliott, 2005. Introduction to Fiber Optics. 3rd Edn., Elsevier, New York, ISBN-13: 9780750667562.

Entezari, E. and H. Golnabi, 2011. Role of fiber arrangements in operation of a double-fiber opto-mechanical system. J. Applied Sci., 11: 3001-3027.

Golnabi, H. and R. Jafari, 2006. Design and performance of an optical fiber sensor based on light leakage. Rev. Sci. Instrum., 77: 1-3.

Haghighatzadeh, A., H. Golnabi and M. Shakouri, 2009. Design and operation of a simple beam shaping system. J. Applied Sci., 9: 3350-3356.

Ieda, K., K. Nakajima, T. Matsui, I. Sankawa and T. Shitaba *et al.*, 2008. Characteristics of bending loss optimized hole assisted fiber. Opt. Fiber Technol., 14: 1-9.

Jafari, R. and H. Golnabi, 2008. Spectral analysis using a new opto-mechanical instrument. J. Applied Sci., 8: 3669-3675.

Jafari, R. and H. Golnabi, 2010. Simulation of three different double-fiber probes for reflection sensing. J. Applied Sci., 10: 20-28.

Khorramnazari A. and H. Golnabi, 2011. Object surface characteristics monitoring using light reflection measurements. J. Applied Sci., 11: 2823-2829.

Levi, L., 1980. Applied Optics: A Guide to Optical System Design. Vol. 2. John Wiley and Sons, New York..

Mohanty, L. and K.S.C. Kuan, 2011. Surface structure monitoring with plastic optical fiber. Opt. Lasers Eng., 49: 984-987.

Nakajima, K., T. Shimizu, T. Matsui, C. Fukai and T. Kurashima, 2010. Single-mode hole-assisted fiber as a bending-loss insensitive fiber. Opt. Fiber Technol., 16: 392-398.

Senior, J.M., 1985. Optical Fiber Communications, Principles and Practice. Prentice-Hall, New York, USA., Pages: 922.

Van Etten, W. and J.V. Plaats, 1991. Fundamentals of Optical Fiber Communications. Prentice-Hall, New York, USA., Pages: 470.

Zubia, J. and J. Arrue, 2001. Plastic optical fibers: An introduction to their technical processes and applications. Opt. Fiber Technol., 7: 101-140.